Estimating wind using a quadrotor

Gautier Hattenberger, Murat Bronz and Jean-Philippe Condomines
ENAC, Université de Toulouse, France
firstname.lastname@enac.fr

ABSTRACT

The aim of this work is to estimate the wind that the quadrotor drone is subject to only based on standard navigation sensors and equations of motion. It can be used in several situation, including atmospheric studies, trajectory planning under environmental constraints, or as a reference for studying flights in shear layer. For this purpose, a small quadrotor drone with spherical shape has been developed. Flight data are recorded from telemetry during indoor and outdoor flight tests and are post-processed. The proposed solution is based on a calibration procedure with global optimization to extract the drag model and a Kalman Filter for online estimation of the wind speed and direction.

1 INTRODUCTION

Estimating wind with a UAV has already been studied with multiple approaches. A common way is to use a fixed-wind aircraft and extract the wind from its GPS track [1] or by adding sensors on the system, such as 5-hole probe [2, 3] or a combination of simple Pitot tube and flags [4].

For a quadrotor, these approaches are not suitable, not only due to the non-constant inclination angles and flight directions, but also because of the low flight speeds. However, [5] compared the use of four different anemometers on a quadrotor. The study revealed that a thermal anemometer could be used, at the cost of modifications to the UAV structure in order to place it far enough from the disturbances induced by propellers.

Instead of adding components on the UAV, an alternate solution is to estimate wind from the quadrotor motion [6, 7, 8, 9]. In [7], the different possible models are presented: static, kinematic or full dynamic. In addition, a methodology to extract the required parameters is presented. The propulsion system is characterized by a motor test bench in a wind tunnel experiment, while the drag is extracted from flights at constant GPS velocity in steady air. The observation is made that the drag is proportional to the relative airspeed. In [6, 10], experiments were led using a six-axis force balance, a very precise but fragile and expensive system. Finally, [8] presents a nonlinear observer able to accurately predict the wind components, using only low cost Inertial Measurement Unit (IMU) and ground speed measurements. The drag-force is considered proportional to the rotational speed of the motors, that is almost constant during operation, leading to a constant rotor drag coefficient, similar to [7, 11]. [9, 7] have performed outdoor flights and compared the results with ground reference measurements, demonstrating the feasibility of wind measurement from quarotor based on IMU and GPS measurements. The general principals and equations of motion from these studies have been used as a starting point for the present article.

This paper is organized as follows. First, the problem modeling focuses on the equations of motion, the hypothesis and limitations, as well as the experimental airframe. Then, the parameters identification method is presented and after that, the wind estimation with a Kalman filter is exposed. Finally, in-flight experiments are described and their results are analyzed.

2 PROBLEM FORMULATION

2.1 Kinematic and Dynamic model

With the assumptions that

- the center of gravity (CG) is located at the center and origin of the body frame
- the frame and the propellers are rigid
- the inputs of the system are the thrust generated by the motors
- the outputs are the position and orientation of the body frame relative to the earth (inertial) frame, observed by the GPS and IMU sensors

a simple dynamic particle model can be established as in [7], leading to:

$$\dot{\mathbf{X}} = \mathbf{V_k} = \mathbf{V_r} + \mathbf{V_w} \tag{1}$$

$$m\dot{\mathbf{V}}_\mathbf{k} = m\mathbf{g} + \mathbf{D}(V_a) + \mathbf{T} \tag{2}$$

where:

- $\mathbf{X}$ is the position vector relative to earth frame
- $\mathbf{V_k}$ is the ground speed vector relative to earth frame (inertial velocity)
- $\mathbf{V_r}$ is the relative air speed vector
- $\mathbf{V_w}$ is the wind speed vector relative to earth frame
- equation 1 represents the wind triangle
- m is the mass of the model and $\mathbf{g}$ the gravity vector

http://www.imavs.org/

http://www.imavs.org/

- $V_a = \|\mathbf{V_r}\|$ is the norm of the airspeed
- **D** is the drag vector in earth frame, as a function of airspeed
- **T** is the control forces vector (thrust) in earth frame

Finally, the last assumption is that the wind speed is seen as a constant or slowly varying disturbance, therefore the derivative of the wind triangle (equation 1) gives:

$$\dot{\mathbf{V}}_\mathbf{w} = 0 \quad \Rightarrow \quad \dot{\mathbf{V}}_\mathbf{k} = \dot{\mathbf{V}}_\mathbf{r} \tag{3}$$

A typical drag equation is expressed as the product of the dynamic pressure, a reference surface and a drag coefficient function of α and β, the the two angles defining the direction of the air velocity relative to the body frame (see Figure 1). As a result, drag should be proportional to V_a^2. However,

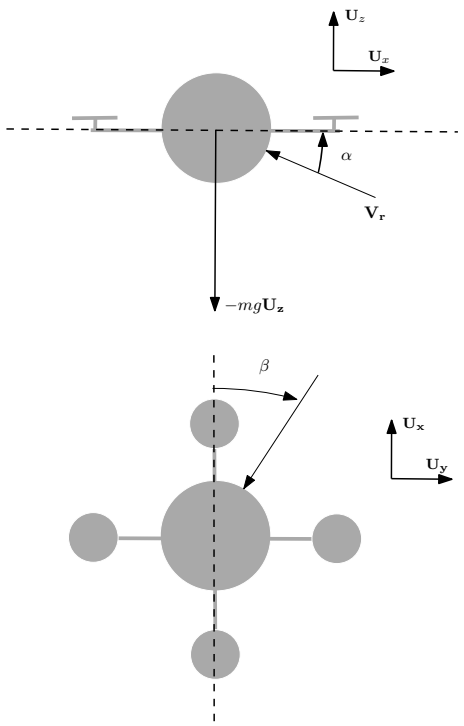

Figure 1: Aerodynamic frame with angle of attack α and side slip angle β

the experimental results presented in the calibration section 3 show that in the range of the considered wind speeds, the rotor drag or H-force (see [11]) that is linear with the airflow seems to be dominant, hence:

$$\|\mathbf{D}\| = k\, V_a \tag{4}$$

As an additional remark, the airframe is not not supposed to generate lift and is symmetrical to reduce the dependency with the direction of the relative airspeed (independent of β).

The control force vector **T** can be expressed from the norm of the thrust T_{total}, assumed to be the sum of each motor thrust applied at the CG, and the orientation of the body relative to earth frame represented by the rotation matrix $\mathbf{R_{0b}}$. This matrix can be computed from Euler angles ϕ, θ and ψ with the classic DCM matrix as in [7].

$$\mathbf{T} = \begin{pmatrix} T_x \\ T_y \\ T_z \end{pmatrix} = \mathbf{R_{0b}}^{-1} \begin{pmatrix} 0 \\ 0 \\ T_{total} \end{pmatrix} \tag{5}$$

2.2 *Airframe characteristics*

A custom quadrotor frame have been designed for this experiment. It is a simple cross shape made of thin aluminum bars to hold the motors and a spherical 3D-printed central body around the electronic components and the battery, as seen on the Figure 2. The reason for this choice is to have a symmetrical shape in order to reduce or eliminate the dependency between the generated drag and the heading of the drone.

The general characteristics and components are summarized in the Table 1. The autopilot software used is the *Paparazzi* UAV System [12].

component	characteristic
material	aluminum & plastic (PLA)
motors	T-motor F30
propellers	Dalprop 5x4 (3 blades)
battery	3S, 2200 mAh
autopilot	Tawaki v1 with Paparazzi
GPS	U-blox M8
size (motor to motor)	47 cm
sphere diameter	22 cm
mass	896 grams
flight time	7 minutes

Table 1: Quadrotor characteristics

Figure 2: Quadrotor with custom spherical body shape

http://www.imavs.org/

3 CALIBRATION METHODOLOGY

Estimating the wind from the quadrotor motion requires to estimate the drag parameters. The methodology applied is similar to [7] with the measurement of the bank angles ϕ and θ at different airspeed. One of the difference is that instead of moving at constant ground speed in steady air, the drone is controlled to stay at the same position in front a *WindShape* wind generator, as seen Figure 3. The calibration is done inside a flight arena at ENAC (École Nationale de l'Aviation Civile, Toulouse, France) also equipped with an *Optitrack* motion capture system. Hence the position and velocity is accurately controlled in closed-loop and the flight can be considered in equilibrium.

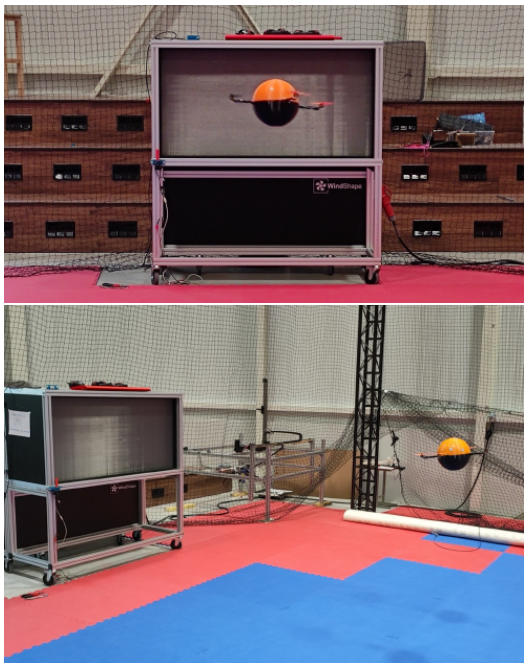

Figure 3: Quadrotor during calibration in from of the WindShape wind generator

The dynamic equation 2 in equilibrium state, illustrated by the Figure 4, directly provides a measurement of the drag force from the bank angle and the mass. Without loss of generality, the vertical component of the thrust compensate the weight and the horizontal thrust compensate the drag:

$$\begin{cases} T_{total}\ cos(\alpha) = T_z = mg \\ T_{total}\ sin(\alpha) = T_x = D_x = \|\mathbf{D}\| \end{cases} \Leftrightarrow mg\ tan(\alpha) = D_x$$

The calibration procedure is as follow:

- start the wind generator and measure the reference wind speed with an anemometer (hot-wire in our case)
- takeoff and place the quadrotor at a distance corresponding to the reference measurement

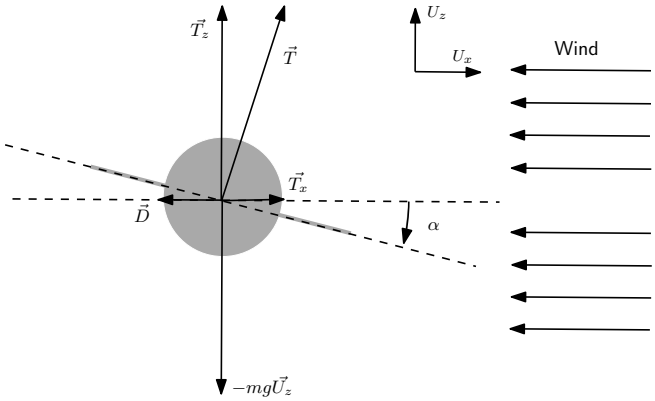

Figure 4: Side view of the forces applied on the quadrotor model in presence of horizontal wind

- when stabilized, change the heading to make one or more full turn on itself
- record the attitude (ϕ, θ, ψ)
- repeat the procedure at a different wind speed

For each reference wind speed, a fitting algorithm is used to map the relation between the bank angles (ϕ or θ) and the heading ψ with a sinusoidal form:

$$\phi \text{ or } \theta = c_1\ sin(c_2\ \psi + c_3) \tag{6}$$

where the coefficient c_1 is the magnitude of the oscillation, equal to the incidence α_{eq} at equilibrium state, c_2 and c_3 are frequency and phase parameters, not used later on. The Figure 5 shows the bank angle ϕ as a function of the heading ψ after a full turn. The rotation is not continuous, but made a 3s steps every after a rotation of 20°. The reference speed for this case is 6.57 m/s, corresponding to a 50% throttle of the wind generator. The curve fitting is done with Matlab and gives the result $c_1 = 0.1274$ with a R-square of 0.9271.

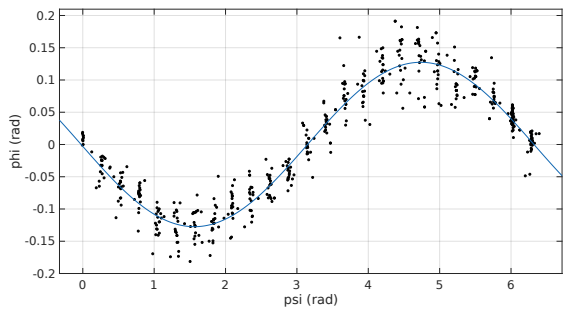

Figure 5: Roll angle ϕ against heading angle ψ after a complete turn in from of the wind generator, the sinusoidal fitting curve is in blue

Similar results are obtained for θ, which confirms this independence of the drag with β, and for the different reference

http://www.imavs.org/

speeds. The final result is presented with the Figure 6 that represents the relation between the angle of attack α_{eq} and the reference air speed. As mentioned in the previous section with equation 4, the relation is linear and the fitting curves gives:

$$tan(\alpha_{eq}) = c_\alpha * V_a$$
$$c_\alpha = 0.0262$$

with a R-square of 0.9998. It gives for our quad model with a mass of 896 grams a coefficient $k = mg * c_\alpha = 0.230$ in equation 4.

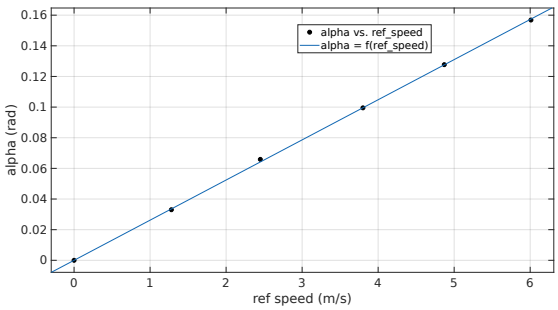

Figure 6: Relation between the incident angle α versus the reference speed measured from a hot-wire airspeed probe at the same distance from the wind generator

4 WIND ESTIMATION WITH KALMAN FILTER

This problem considers simultaneous estimation of $2D$ aircraft Earth-axis velocity $\mathbf{V_r} = (V_{r_x}, V_{r_x})$ and wind velocity components (V_{w_x}, V_{w_y}). Both process and measurement equations are dependent on aerodynamic force described above. The attitude and heading estimation (AHRS filter) is performed through a fusion algorithm of low-cost inertial sensors used for UAV navigation.

All the sensors embedded are low-cost, and therefore have imperfections. The major error sources in the navigation system are due to: - all of the disturbances (noises) that affect the instruments; - the potential incorrect navigation system initialization (e.g. on magnetometers sensor); - and the inadequacy between the real local Earth's gravity value and the one used for computation. The largest error is usually a bias instability (expressed respectively in deg/hr for gyros and μg for the accelerometers). All these measurements are obviously corrupted by additive noises for which it appears reasonable to assimilate their stochastic properties to the ones of Gaussian processes. Their covariances matrices have been identified in [13].

Using these values, the state space representation corresponding to $\mathscr{M}_s$ can be described in a linear form:

$$\dot{\mathbf{x}} = A\mathbf{x} + B\mathbf{u} + \nu \qquad \text{and} \qquad \mathbf{y} = C\mathbf{x} + \mu$$

where: $\mathbf{x} = [V_{r_x}, V_{w_x}, V_{r_y}, V_{w_y}]^T$, $\mathbf{u} = [T_x, T_y]$ and $\mathbf{y} = [V_{k_x}, V_{k_y}]^T$ are the state, input and output vectors respectively. Moreover, ν, μ are the zero-mean Gaussian process noise vectors with covariance matrix, Q, R.

$$\mathscr{M}_s \begin{cases} \dot{\mathbf{x}} = \begin{pmatrix} \frac{-k}{m} & 0 & 0 & 0 \\ 0 & 0 & 0 & 0 \\ 0 & 0 & \frac{-k}{m} & 0 \\ 0 & 0 & 0 & 0 \end{pmatrix} \mathbf{x} + \begin{pmatrix} \frac{1}{m} & 0 \\ 0 & 0 \\ 0 & \frac{1}{m} \\ 0 & 0 \end{pmatrix} \mathbf{u} + \nu \\ \\ \begin{pmatrix} V_{k_x} \\ V_{k_y} \end{pmatrix} = \begin{pmatrix} 1 & 1 & 0 & 0 \\ 0 & 0 & 1 & 1 \end{pmatrix} \mathbf{x} + \mu \end{cases}$$

Obviously, to implement these equation a discrete form is used such that :

$$\begin{cases} \mathbf{x}_{k+1} = A_d \mathbf{x}_k + B_d \mathbf{u}_{k-1} + \nu_k \\ y_k = C_d \mathbf{x}_k + \mu_k \end{cases}$$

where $A_d = \exp(Adt)$,$B_d = \int_0^{dt} \exp(A\xi) B d\xi$,$C_d = C$ are the discrete-time state matrices and dt is the sampling time of the system. Process and measurement equations becomes :

$$\mathscr{M}_d \begin{cases} \begin{pmatrix} V_{r_x} \\ V_{w_x} \\ V_{r_y} \\ V_{w_y} \end{pmatrix}_{k+1} = \begin{pmatrix} 1 - \frac{kdt}{m} & 0 & 0 & 0 \\ 0 & 1 & 0 & 0 \\ 0 & 0 & 1 - \frac{kdt}{m} & 0 \\ 0 & 0 & 0 & 1 \end{pmatrix} \mathbf{x}_k + \dots \\ \qquad \begin{pmatrix} \frac{dt}{m} - \frac{kdt^2}{2m^2} & 0 \\ 0 & 0 \\ 0 & \frac{dt}{m} - \frac{kdt^2}{2m^2} \\ 0 & 0 \end{pmatrix} \mathbf{u}_{k-1} + \nu_k \\ \\ \begin{pmatrix} V_{k_x} \\ V_{k_y} \end{pmatrix}_k = \begin{pmatrix} 1 & 1 & 0 & 0 \\ 0 & 0 & 1 & 1 \end{pmatrix} \mathbf{x}_k + \mu_k \end{cases}$$

Computing the rank of the observability matrix shows that the system is fully observable at all speed. It can be mentioned this results from the linear relation of drag with airspeed in equation 4. The case of a sphere without propellers in a airflow would give a drag as the square of the airspeed and a loss of observability at the zero airspeed, in addition with the need of an Extended Kalman filter form.

In the later experiments, the process noise relative to airspeed evolution is $\nu_{V_a} = 0.05$, the process noise relative to windspeed evolution is $\nu_{V_w} = 0.001$ and the sensor noise associated to ground speed measurement is $\mu_{V_k} = 0.1$. Second order terms (in dt^2) can be neglected.

5 EXPERIMENTAL FLIGHTS

5.1 *Indoor flight in controlled wind speed*

The wind estimation algorithm is first evaluated with a flight indoor in front of the wind generator used for calibra-

http://www.imavs.org/

tion. The goal is to evaluate the stability and convergence of the estimation in a controlled environment. In this setup, the wind is coming from a virtual north and the quadrotor is hovering at a fixed position. Ground speed and orientation are recorded from the telemetry and post-process by the Kalman filter in a Matlab script.

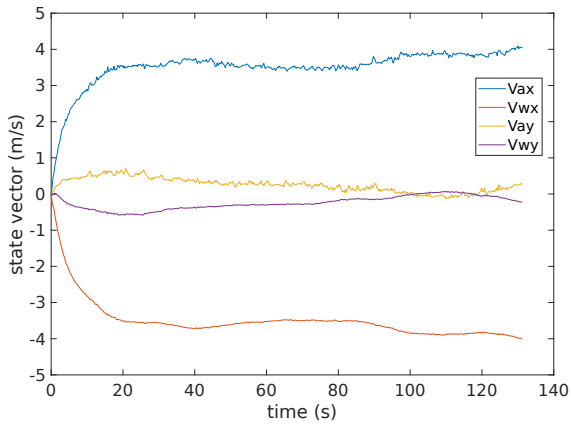

Figure 7: Evolution of the Kalman filter state vector over time during indoor flight

The Figure 7 shows the four elements of the state vector. The convergence time is around 10 to 20 seconds. The noise on the estimated airspeed is low thanks to the low noise on the measured ground speed (from motion capture) and the stable airflow.

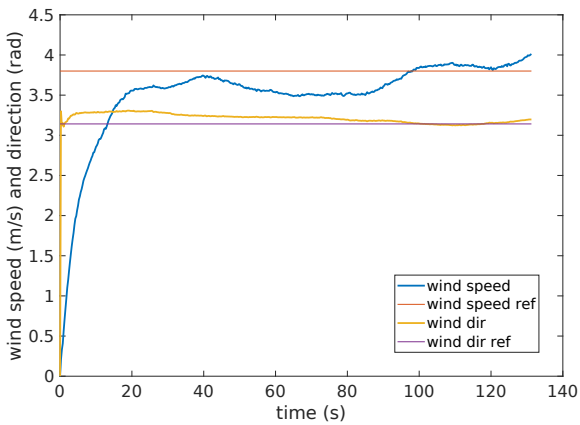

Figure 8: Wind speed and direction compared to the reference value from the wind generator; wind is coming from a virtual north (π rad) at a speed of 3.8 m/s

The Figure 8 is the norm of the estimated wind speed $\|\mathbf{V_w}\| = \sqrt{V_{w_x}^2 + V_{w_y}^2}$ and the wind direction. During this experiment, the wind generator throttle was set to 40%, corresponding to 3.8 m/s at the location of hovering with a direction of 180°. As we can see on this plot, the estimated wind converges to the reference values. The response time for the direction is much faster than for the norm of the speed. This can be explained by the fact that our model states that the wind has a very slow evolution. Since the initial condition for the state vector is zero, it takes some time to reach the final value, but even if the norm is not yet correct, the direction of the wind is already valid.

5.2 *Outdoor flights*

Several flights have been performed outdoor to record telemetry data, with attitude from IMU and this time ground speed from real GPS sensor. Only two relevant flights are presented in this paper. They were performed at Muret's model airfield (close to Toulouse, France) on the 20th of May 2021. The wind conditions for that day are coming from public meteorological data and are reported in Table 2.

time	speed	direction
9 am	no wind	N/A
10 am	7.4 km/h (2.06 m/s)	110°
11 am	9.3 km/h (2.58 m/s)	120°
12 am	9.3 km/h (2.58 m/s)	70°

Table 2: Wind condition on the day of the outdoor experiment

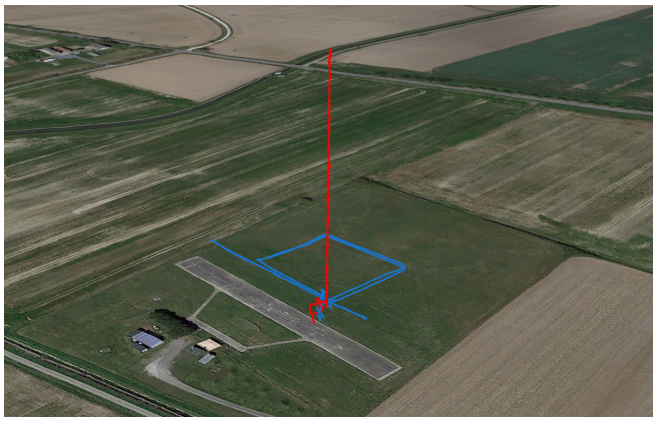

Figure 9: Trajectories for the outdoor flights: vertical profile in red, horizontal square at constant altitude in blue

The first flight corresponds to the vertical profile (red trajectory on Figure 9). The quadrotor goes up and down at a vertical speed of 1 m/s and with the heading changing at constant rate. The horizontal speed is close to zero. The state vector evolution is plotted on Figure 10. As expected, the noise on airspeed estimate is stronger than during indoor experiment due to sensor noise, but still acceptable.

The vertical flight was done a bit after 10 am, so according to Table 2 between 2 and 2.5 m/s, with a direction between 110° and 120°. The speed of 2.2 m/s and the direction of 115° have been kept as a reference. The Figure 11 shows

http://www.imavs.org/

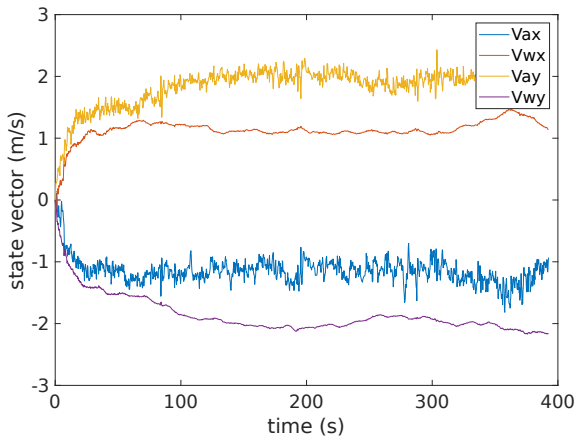

Figure 10: Evolution of the Kalman filter state vector over time during outdoor flight (vertical profile)

the norm and direction of the estimated wind compared to these reference values. It can be seen that both values are converging smoothly to the expected values.

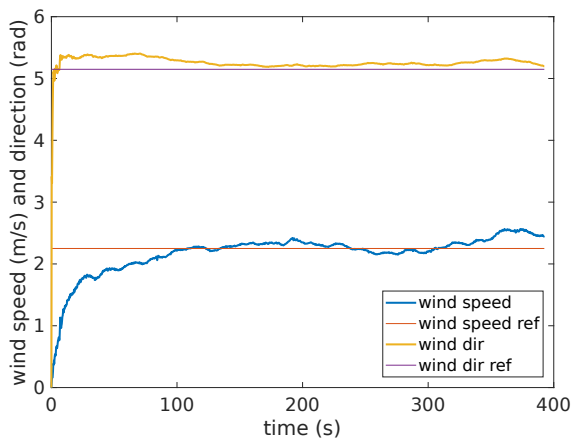

Figure 11: Wind speed and direction compared to the reference value from public meteo data during the outdoor flight (vertical profile)

The second flight is a square (blue trajectory on Figure 9) at low altitude. As a consequence, the ground speed is changing, with horizontal acceleration when changing direction. These variations can be seen in the airspeed vector on Figure 12. The wind vector is also showing some variations and is less stable than with the previous case.

The square flight was done at 9:30, so according to Table 2 between 0 and 2 m/s, with a direction around 110°. The reference speed of 1 m/s have been kept. The norm and direction are still converging, but with more variations due to the changes in ground speed as mentioned before. Nevertheless, all parameters stay in acceptable range and provide a valid

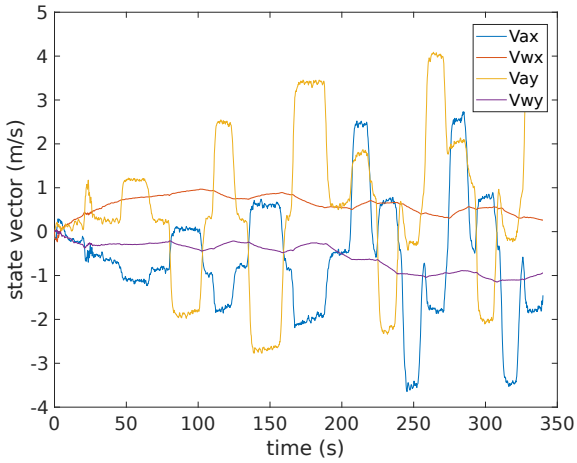

Figure 12: Evolution of the Kalman filter state vector over time during outdoor flight (square trajectory)

estimation of the wind components.

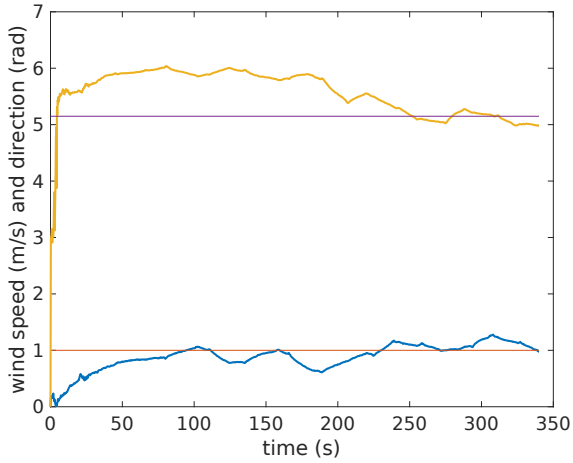

Figure 13: Wind speed and direction compared to the reference value from public meteo data during the outdoor flight (square trajectory)

6 CONCLUSION

A wind estimation filter based on the orientation and ground speed of a quadrotor have been presented. Experimental flights were conducted to compute the calibration parameters of the model and validate the results in controlled indoor flight, as well as outdoor conditions.

The next step is the implementation of the Kalman filter in the flight controller of the autopilot to provide real-time estimation on-board. Such information can be useful to improve navigation or even state estimation.

ACKNOWLEDGEMENTS

This work have been done using the preliminary work and calibration experiments of Laurent Hublet, Maxime Vacheron and Carl Guilly, students at Enac, during their second year project under the supervision of the authors.

REFERENCES

[1] Stéphanie Mayer, Gautier Hattenberger, Pascal Brisset, Marius Jonassen, and Joachim Reuder. A "no-flow-sensor" wind estimation algorithm for unmanned aerial systems. *International Journal of Micro Air Vehicles*, 4(1):pp 15–30, March 2012.

[2] A. C. Kroonenberg, T. Martin, M. Buschmann, J. Bange, and P. Vörsmann. Measuring the wind vector using the autonomous mini aerial vehicle m2av. *Journal of Atmospheric and Oceanic Technology*, 25:1969–1982, 2008.

[3] S. Prudden, A. Fisher, M. Marino, A. Mohamed, S. Watkins, and G. Wild. Measuring wind with small unmanned aircraft systems. *Journal of Wind Engineering and Industrial Aerodynamics*, 176:197–210, 2018.

[4] Jean-Philippe Condomines, Murat Bronz, Gautier Hattenberger, and Jean-François Erdelyi. Experimental Wind Field Estimation and Aircraft Identification. In *IMAV 2015: International Micro Air Vehicles Conference and Flight Competition*, Aachen, Germany, September 2015.

[5] Carl A. Wolf, Richard P. Hardis, Steven D. Woodrum, Richard S. Galan, Hunter S. Wichelt, Michael C. Metzger, Nicola Bezzo, Gregory C. Lewin, and Stephan F.J. de Wekker. Wind data collection techniques on a multi-rotor platform. In *2017 Systems and Information Engineering Design Symposium (SIEDS)*, pages 32–37, 2017.

[6] Fabrizio Schiano, Javier Alonso-Mora, Konrad Rudin, Paul Beardsley, Roland Siegwart, and Bruno Sicilianok. Towards estimation and correction of wind effects on a quadrotor uav. In *IMAV 2014 : International Micro Air Vehicle Conference and Competition 2014*, pages 134 – 141, Delft, 2014. International Micro Air Vehicle Conference and Competition 2014 (IMAV 2014). International Micro Air Vehicle Conference and Competition 2014 (IMAV 2014); Conference Location: Delft, Netherlands; Conference Date: August 12-15, 2014.

[7] Javier González-Rocha, Craig A. Woolsey, Cornel Sultan, and Stephan F. J. De Wekker. Sensing wind from quadrotor motion. *Journal of Guidance, Control, and Dynamics*, 42(4):836–852, 2019.

[8] L.N.C. Sikkel, G.C.H.E. de Croon, C. De Wagter, and Q.P. Chu. A novel online model-based wind estimation approach for quadrotor micro air vehicles using low cost mems imus. In *2016 IEEE/RSJ International Conference on Intelligent Robots and Systems (IROS)*, pages 2141–2146, 2016.

[9] Patrick P. Neumann and Matthias Bartholmai. Real-time wind estimation on a micro unmanned aerial vehicle using its inertial measurement unit. *Sensors and Actuators A: Physical*, 235:300–310, 2015.

[10] Matthew Marino, Alex Fisher, Reece Clothier, Simon Watkins, Samuel Prudden, and Chung Sing Leung. An evaluation of multi-rotor unmanned aircraft as flying wind sensors. *International Journal of Micro Air Vehicles*, 7(3):285–299, 2015.

[11] Robert C. Leishman, John C. Macdonald, Randal W. Beard, and Timothy W. McLain. Quadrotors and accelerometers: State estimation with an improved dynamic model. *IEEE Control Systems Magazine*, 34(1):28–41, 2014.

[12] Gautier Hattenberger, Murat Bronz, and Michel Gorraz. Using the Paparazzi UAV System for Scientific Research. In *IMAV 2014, International Micro Air Vehicle Conference and Competition 2014*, pages pp 247–252, Delft, Netherlands, August 2014.

[13] Murat Bronz, Jean-Philippe Condomines, and Gautier Hattenberger. Development of an 18cm Micro Air Vehicle : QUARK. In *IMAV 2013, International Micro Air Vehicle Conference and Flight Competition*, Toulouse, France, September 2013.

http://www.imavs.org/